

FKPP equation with impulses on unbounded domain

Valaire Yatat, Yves Dumont

Abstract This paper deals with the problem of travelling wave solutions in a scalar impulsive FKPP-like equation. It is a first step of a more general study that aims to address existence of travelling wave solutions for systems of impulsive reaction-diffusion equations that model ecological systems dynamics such as fire-prone savannas. Using results on scalar recursion equations, we show existence of populated vs. extinction travelling waves invasion and compute an explicit expression of their spreading speed (characterized as the minimal speed of such travelling waves). In particular, we find that the spreading speed explicitly depends on the time between two successive impulses. In addition, we carry out a comparison with the case of time-continuous events. We also show that depending on the time between two successive impulses, the spreading speed with pulse events could be lower, equal or greater than the spreading speed in the case of time-continuous events. Finally, we apply our results to a model of fire-prone grasslands and show that pulse fires event may slow down the grassland vs. bare soil invasion speed.

Valaire Yatat

Department of Mathematics, Faculty of Science, University of Yaoundé I, Yaoundé, Cameroon
IRD, UMI 209, UMMISCO, IRD France Nord, F-93143 Bondy, France
e-mail: yatat.valaire@gmail.com

Yves Dumont

CIRAD, UMR AMAP, Pretoria, South Africa
AMAP, Univ. Montpellier, CIRAD, CNRS, INRA, IRD, Montpellier, France
Department of Mathematics and Applied Mathematics, University of Pretoria, South Africa
e-mail: yves.dumont@cirad.fr; yves.dumont@up.ac.za

Citation: Valaire Yatat, Yves Dumont, FKPP equation with impulses on unbounded domain, in R. Anguelov, M. Lachowicz (Editors), *Mathematical Methods and Models in Biosciences*, Biomath Forum, Sofia, 2018, <http://dx.doi.org/10.11145/texts.2017.11.157>

Copyright: © 2018 Yatat et al. This article is distributed under the terms of the Creative Commons Attribution License (CC BY 4.0), which permits unrestricted use, distribution, and reproduction in any medium, provided the original author and source are credited.

1 Introduction

Mathematical models have long been central to the development of spatial theory in ecology (e.g. Shigesada and Kawasaki (1997) [33], Okubo and Levin (2001) [23], Volpert (2014) [43], Logan (2008) [20], (2015) [21], Perthame (2015) [25]). Mathematical literature that deals with species spread mostly relies on reaction-diffusion equations. Reaction-diffusion equations assume that dispersal is governed by random diffusion and that dispersal and growth take place continuously in time and space (Lewis and Li (2012) [19]). They have had remarkable success in explaining the rates at which species have invaded large open environments (Shigesada and Kawasaki (1997) [33], Okubo and Levin (2001) [23], Lewis and Li (2012) [19], Volpert (2014) [43], Logan (2008) [20], (2015) [21], Perthame (2015) [25]).

A simple and classic reaction-diffusion equation that presents population invasion phenomenon is the so-called FKPP (Fisher, Kolmogorov, Petrowsky and Piskounov) equation studied by Fisher (1937) [12] and Kolmogorov et al. (1937) [17]. It consists on adding a diffusion term to the logistic growth term (Fisher (1937) [12], Kolmogorov et al. (1937) [17]). The FKPP equation can model several ecological resources dynamics. Moreover, it is well-known that ecological resource may experience several phenomena that can be either time-continuous (growth, death, birth, release, etc.) or time-discrete (harvest, birth, death, release, etc.) (e.g. Ma and Li (2009) [22], Dumont and Tchuente (2012) [10]). Therefore, a major question is to characterize the impact of such phenomena (time-continuous or not) on the whole dynamic of the system.

This paper deals with the FKPP equation on unbounded domain with time-continuous as well as time-discrete (impulsive) phenomena. The aim is to assess the impact of such phenomena in the system dynamics. This paper is the first step of a more general study that aims to characterize existence of travelling wave solutions for systems of impulsive reaction-diffusion equations. Impulsive reaction-diffusion equations can be used to model ecological systems dynamics such as fire-prone savannas. Readers are referred to Yatat et al. (2017b) [46] for travelling waves in savanna reaction-diffusion models with time-continuous fire events. To the best of authors' knowledge, existence of travelling wave solutions for system of impulsive reaction-diffusion equations is not well documented except in Huang et al. (2017) [14]. The rest of the paper is organized as follows. In the next section (section 2), we present the FKPP model taking into account either time-continuous or both time-continuous and time-discrete events. In section 3 we present result on the existence of spreading speed and traveling wave solutions for the model, and provide a formula for the spreading speed. In section 4, we apply our result for the case of fire-prone grasslands. Section 5 deals with simulations for the models. Section 6 includes some concluding remarks and discussions.

2 Models formulation

The FKPP model in bounded domain without any perturbations (Fisher (1937) [12], Kolmogorov et al. (1937) [17]) reads as

$$\frac{\partial G}{\partial t} = \gamma \left(1 - \frac{G}{K}\right) G + D \frac{\partial^2 G}{\partial x^2} \quad (1)$$

where $t \geq 0$ and x belongs to the one-dimension spatial domain $\Omega = (0, d)$, $0 < d < +\infty$. G is the state variable, γ is the intrinsic growth rate while K is the state variable carrying capacity. The initial data is given by

$$0 \leq G(0, x) = G_0(x). \quad (2)$$

In addition, we also consider homogeneous Neuman boundary conditions for the state variable, i.e.,

$$\frac{\partial G(t, x)}{\partial x} = 0 \quad \text{at} \quad x = 0 \quad \text{and} \quad x = d. \quad (3)$$

However and as it was previously discussed, the state variable G can experience several perturbations. In the case where all perturbations are taken into account as time-continuous events, model (1) could read as

$$\frac{\partial G}{\partial t} = \gamma \left(1 - \frac{G}{K}\right) G - (\mu + f\eta)G + D \frac{\partial^2 G}{\partial x^2} \quad (4)$$

where, for example, μ may denote the natural death rate. The term $f\eta$ could represent a death rate as a consequence of harvesting. In this case, f is the harvest frequency while η is the constant proportion of the state variable which is removed during the harvest. Conversely, if we suppose that perturbations that impact system (1) are divided in two groups: those who can be taken into account as time-continuous events (e.g. natural death) and those who may be considered as time-discrete (e.g. harvest), then model (4) could be rewritten as follow

$$\begin{cases} \frac{\partial G}{\partial t} = \gamma \left(1 - \frac{G}{K}\right) G - \mu G + D \frac{\partial^2 G}{\partial x^2} & t \neq t_k, \\ G(t_k^+, x) = (1 - \eta)G(t_k, x), & t = t_k, t_{k+1} = t_k + \tau \end{cases} \quad (5)$$

where $t_k^+ = \lim_{\theta \rightarrow 0^+} (t_k + \theta)$ is the time just after the harvest, $k = 1, 2, 3, \dots$, $t \geq 0$, $x \in \Omega$ and equations (2)-(3) still hold. In model (5), τ is the time between two successive harvest events and $\tau = 1/f$ where f is the harvest frequency.

Existence, unicity, positivity and boundedness of solutions of problem (4)-(2)-(3) follow directly from Proposition 1, Lemma 2 and Proposition 2 of Yatat et al. (2017b) [46]. Similarly, existence and unicity of solutions of problem (5)-(2)-(3) hold according to [Rogovchenko (1997a) [28], Theorem 2.1, Rogovchenko (1997b) [27], Theorem 2.2] while positivity and boundedness follows from Lemma 2 of

Yatat et al. (2017b) [46] (see also Corollary 3.3 of Kiriane and Rogovchenko (1997) [16], Lemma 1 of Yatat et al. (2017) [47]).

Before going further, let us make some comments about how impulsive phenomena are taken into account in mathematical models. Actually, there exist several possibilities including the formalism presented in system (4) (see also Lakshmikantham et al. (1989) [18], Bainov and Simeonov (1995) [4], Dumont and Tchuente (2012) [10], Dufourd and Dumont (2013) [9], Tchuente Tamen et al. (2016) [35], (2017) [36], Yatat et al. (2017) [47] and references therein) as well as the formalism advocated by Lewis and Li (2012) [19] (see also Vasilyeva et al. (2012) [42], Fazly et al. (2017) [11], Huang et al. (2017) [14] and references therein). For τ -periodic impulsive harvest events, the inter-harvest saison (i.e. the time between two successive harvest events) has a length of τ (units of time) and at the end of the inter-harvest saison, harvest occurs. Thus one can consider the whole time interval as a succession of inter-harvest saisons of length τ . Let us denote the state variable at time $t \in [0, \tau]$ and location x during the inter-harvest saison n as $G_n(t, x)$. Following Lewis and Li (2012) [19], system (5) reads as

$$\begin{cases} \frac{\partial G_n}{\partial t} = \gamma \left(1 - \frac{G_n}{K}\right) G_n - \mu G_n + D \frac{\partial^2 G_n}{\partial x^2}, \\ G_{n+1}(0, x) = (1 - \eta) G_n(\tau, x), \quad x \in \Omega, t \in (0, \tau). \end{cases} \quad (6)$$

We also consider initial and boundary conditions given by equations (2) and (3), respectively. The discrete updating function from the beginning of one inter-harvest saison to the next is

$$G_{n+1}(0, x) = \mathcal{Q}_\tau(G_n(0, x)) = \mathcal{Q}_\tau[G_n](x) \quad (7)$$

where \mathcal{Q}_τ is the time- τ -map of the reaction-diffusion equation of system (6) (i.e., the first equation of (6)).

In the sequel we discuss the problem of minimal domain size when homogeneous Dirichlet boundary condition (DBC) are considered instead of homogeneous Neuman boundary condition given in (3). The homogenous DBC is given by

$$G(t, 0) = G(t, d) = 0, \quad t \geq 0. \quad (8)$$

In the following lemma we will distinguish two cases: time-continuous harvest and time-discrete harvest.

Lemma 1. (*Dirichlet boundary condition and minimal domain size*)

1. *Time-continuous harvests.* Let us set

$$\mathcal{R}^{cont.} = \frac{\gamma}{\mu + f\eta}.$$

When $\mathcal{R}^{cont.} > 1$, we define

$$l_{cont.}^* = \pi \sqrt{\frac{D}{(\mu + f\eta)(\mathcal{R}^{cont.} - 1)}}.$$

Therefore,

a. if $l < l_{cont.}^*$, then the solution $G(t, x)$ of (4)-(2)-(8) satisfies

$$\lim_{t \rightarrow +\infty} G(t, x) = 0. \quad (9)$$

b. if $l > l_{cont.}^*$, then (4)-(2)-(8) admits a positive equilibrium $\bar{G}(x)$, such that

$$\lim_{t \rightarrow +\infty} G(t, x) = \bar{G}(x). \quad (10)$$

Note that, when $\mathcal{R}^{cont.} < 1$, (9) holds. That is, the population cannot persist in space no matter how big l is.

2. Time-discrete harvests. Let us set

$$\mathcal{R} = \frac{\gamma}{\mu}, \quad \mathcal{R}_\tau = (1 - \eta) \exp(\mu(\mathcal{R} - 1)\tau).$$

When $\mathcal{R} > 1$ and $\mathcal{R}_\tau > 1$, we define

$$l_{imp.}^* = \pi \sqrt{\frac{D}{\ln(1 - \eta) + \mu(\mathcal{R} - 1)\tau}}.$$

Therefore,

a. if $l < l_{imp.}^*$, then the solution $G_n(\tau, x)$ of (6)-(2)-(8) satisfies

$$\lim_{n \rightarrow +\infty} G_n(\tau, x) = 0. \quad (11)$$

b. if $l > l_{imp.}^*$, then (6)-(2)-(8) has a minimal positive equilibrium $\bar{G}(x)$, and if $G_0(x)$ is positive on an open subinterval of $(0, l)$, then the solution sequence $G_n(\tau, x)$ satisfies

$$\lim_{n \rightarrow +\infty} \inf G_n(\tau, x) \geq \bar{G}(x). \quad (12)$$

In addition, if $\mathcal{R} < 1$ or $\mathcal{R}_\tau < 1$, then (11) holds (see also Lemma 3).

Proof. See Appendix 6, page 20.

In the next section, we study the nonlinear model (6) on unbounded domain (i.e. $\Omega = \mathbb{R}$) and use the theory developed in Weinberger (1982) [45] to prove the existence and linear determinacy of the spreading speed, and the equivalence of these spreading speeds with the minimum travelling wave speeds.

3 Mathematical analysis on unbounded domain

Non-spatial solutions of (6) satisfy

$$\begin{cases} \frac{du_n}{dt} = \gamma \left(1 - \frac{u_n}{K}\right) u_n - \mu u_n, & t \in (0, \tau), \\ u_{n+1}(0) = (1 - \eta)u_n(\tau). \end{cases} \quad (13)$$

Straightforward computations lead to

Lemma 2. *The solution $u_{n+1} := u_{n+1}(\tau)$ of system (13) is given by*

$$u_{n+1} = \frac{K(\mu - \gamma)(1 - \eta)u_n}{(K(\mu - \gamma) + \gamma(1 - \eta)u_n)e^{(\mu - \gamma)\tau} - \gamma(1 - \eta)u_n}. \quad (14)$$

Thus, the solution of system (13) given by equation (14) generates a discrete dynamical system. Homogeneous equilibria of system (6) are equilibria of model (14). Model (14) always has the trivial equilibrium $e_0 = 0$. Recall that

$$\mathcal{R} = \frac{\gamma}{\mu}, \quad \mathcal{R}_\tau = (1 - \eta) \exp(\mu(\mathcal{R} - 1)\tau).$$

Since $0 \leq 1 - \eta \leq 1$ one has

$$\mathcal{R} < 1 \Rightarrow \mathcal{R}_\tau < 1. \quad (15)$$

The following result is valid

Lemma 3. *1. When $\mathcal{R} < 1$ or $\mathcal{R}_\tau < 1$, the trivial equilibrium $e_0 = 0$ of model (14) is globally asymptotically stable (GAS). That is, $\lim_{n \rightarrow +\infty} u_n(\tau) = 0$.*
2. When $\mathcal{R} > 1$ and $\mathcal{R}_\tau > 1$, system (6) or model (14) has the positive equilibrium

$$e_u = \frac{K(\mathcal{R} - 1)(\mathcal{R}_\tau - 1)}{\mathcal{R}(\mathcal{R}_\tau - 1 + \eta)} \quad (16)$$

which is GAS.

Proof. See Appendix B, page 20.

Actually, the requirement $\mathcal{R}_\tau > 1$ is necessary for the population described by (6) to grow and spread in space. In fact, let $G_n(\tau, x)$ be a solution of (6) with $G_0(\tau, x)$ bounded above by a constant $u_0 < e_u$. Then the comparison theorem for parabolic systems based on the maximum principle (see chapter 3 of Protter and Weinberger (1984) [26]) shows that the solution $G_n(\tau, x)$ of (6) and the solution of $u_n(\tau)$ of (13) satisfy $G_n(\tau, x) \leq u_n(\tau)$. Consequently, when $\mathcal{R}_\tau < 1$ and following Lemma 3, $G_n(\tau, x)$ approaches zero uniformly in $x \in \mathbb{R}$ as $n \rightarrow \infty$.

In the sequel (see Remark 1), we provide some comments between the two formalism described by (5) and (6) without the spatial component.

Remark 1. In Yatat et al. (2017) [47], we solved system (5) without the spatial component and obtained a positive and periodic solution. Indeed, for $t \in (n\tau, (n+1)\tau)$ we found the positive and periodic solution (see Lemma 2, Yatat et al. (2017) [47])

$$V(t) = \frac{K(\mathcal{R} - 1)(\mathcal{R}_\tau - 1)}{\mathcal{R}(\mathcal{R}_\tau - 1 + \eta \exp(-\mu(\mathcal{R} - 1)(t - (n+1)\tau)))} \quad (17)$$

whenever $\mathcal{R} > 1$ and $\mathcal{R}_\tau > 1$. A direct comparison allows us to observe that the positive equilibrium of model (13) given by (14) corresponds to the value of the positive periodic solution (17) computed at $t = (n+1)\tau$, i.e. $V((n+1)\tau)$. This observation reinforces the fact that there exists a direct link between the two aforementioned modelling options of periodic impulsive events.

In the sequel we provide a result that address the travelling wave problem for model (6). Indeed, we show that if $\mathcal{R}_\tau > 1$ holds, then model (6) has a positive asymptotic spreading speed, and the spreading speed can be characterized as the slowest speed of a class of traveling wave solutions. Applying results of Weinberger (1982) [45] (Theorems 6.1-6.6) to the scalar system of recursion (7) as well as results of Lewis and Li (2012) [19] (Theorem 2.1), the following result holds.

Theorem 1. *Suppose that $\mathcal{R}_\tau > 1$ is valid. Then*

$$c_{imp}^* = c^* = 2\sqrt{D(\ln(1-\eta) + \mu(\mathcal{R} - 1))\tau} \quad (18)$$

is the spreading speed of system (6) in the following sense: if the continuous initial function is zero outside a bounded interval, $G_0(0, x) \neq 0$, and $0 \leq G_0(0, x) < e_u$, then for any positive ε the solution $G_n(\tau, x)$ of (6) has the following properties:

1.

$$\lim_{n \rightarrow +\infty} \sup_{|x| \geq n(c^* + \varepsilon)} G_n(\tau, x) = 0. \quad (19)$$

2.

$$\lim_{n \rightarrow +\infty} \sup_{|x| \leq n(c^* - \varepsilon)} (e_u - G_n(\tau, x)) = 0. \quad (20)$$

Furthermore, for $c \geq c^$, system (6) has a continuous nonincreasing traveling wave $w_c(x - nc)$ with $w_c(-\infty) = e_u$ and $w_c(+\infty) = 0$. A continuous nonnegative traveling wave solution $w_c(x - nc)$ in (6) with $w_c(\infty) = 0$ and $\liminf_{x \rightarrow -\infty} w_c(x) > 0$ does not exist if $c < c^*$.*

Proof. The proof of Theorem 1 is using Theorem 2.1 in Lewis and Li (2012) [19], with $g(x) = (1 - \eta)x$.

The properties (19) and (20) indicate that if $G_n(\tau, x)$ is a solution of (6) with nonzero initial data which vanishes outside a bounded interval, then an observer who travels to the left or right with speed greater than c^* will eventually see G_n going to 0, while an observer who travels with a speed below c^* will eventually see G_n approaching e_u .

Theorem 1 further shows that c^* is also the slowest speed of traveling wave solutions connecting 0 with e_u .

Considering time-continuous harvesting as in model (4), the positive equilibrium is

$$E_u = K \left(1 - \frac{1}{\mathcal{R}^{cont.}} \right)$$

where

$$\mathcal{R}^{cont.} = \frac{\gamma}{\mu + f\eta} > 1.$$

Moreover, when $\mathcal{R}^{cont.} > 1$ the spreading speed of traveling wave solutions connecting 0 with E_u is (see also Volpert (2014) [43], Logan (2008) [20], (2015) [21], Perthame (2015) [25], Yatat et al. (2017b) [46] and references therein)

$$c_{cont.}^* = 2\sqrt{D(\mu + f\eta)(\mathcal{R}^{cont.} - 1)}. \quad (21)$$

Recall that with time-continuous events, the study of travelling wave solutions for system (4) is done by considering a 'moving coordinate' $z = x - ct$ where c denotes the wave speed. However for impulsive reaction-diffusion equations written as in equation (5), such moving coordinate is not helpful. Therefore, alternative formulations of impulsive reaction-diffusion equations is needed e.g. formulation presented in (6).

In addition,

$$(c_{imp.}^*)^2 - (c_{cont.}^*)^2 = 4D \left(\ln(1 - \eta) + \frac{\eta}{\tau} + (\gamma - \mu)(\tau - 1) \right). \quad (22)$$

Thus, compared c^* and $c_{cont.}^*$ is equivalent to compute the sign of the function q defined by

$$q(\tau) = \ln(1 - \eta) + \frac{\eta}{\tau} + (\gamma - \mu)(\tau - 1). \quad (23)$$

Specifically,

- $q(\tau) > 0 \Rightarrow c_{imp.}^* > c_{cont.}^*$, i.e. populated vs. extinction travelling waves spreading speed with impulsive harvest is greater than the spreading speed with time-continuous harvest events.
- $q(\tau) = 0 \Rightarrow c_{imp.}^* = c_{cont.}^*$, i.e. with either impulsive and time-continuous harvest events, populated vs. extinction travelling waves have the same spreading speed.
- $q(\tau) < 0 \Rightarrow c_{imp.}^* < c_{cont.}^*$, i.e. spreading speed of populated vs. extinction travelling waves with impulsive harvests is lower than the spreading speed with time-continuous harvest events.

4 Application to fire-prone grasslands

Grassy biomes include grassland and savanna with more or less tree cover (Bond and Parr (2010) [5]). Savannas and grasslands dominate the terrestrial tropics and

cover approximately 20% of the global land surface (Scholes and Archer (1997) [31], Parr et al. (2014) [24]). Tropical grassy biome (TGB) range from open grassland to densely canopied savanna with up to 80% tree cover (Sankaran et al. (2005) [29]). TGB have attracted little of the public interest and conservation attention given to tropical forests. Indeed, according to Bond and Parr (2010) [5], the lack of interest in tropical grassy biomes is highlighted by Web of Science searches (years: 2004-2009; databases: SCI-EXPANDED, CPCI-S) using the search terms 'biodiversity' and 'tropical' with either 'forest*', 'grassland*' or 'savanna*'. Bond and Parr (2010) [5] search revealed 1343 papers on tropical forests, and only 61 and 103 papers on grassland and savanna systems respectively. Using 'conservation' instead of 'biodiversity' as a search term, confirmed their finding with more than eight times as many papers on tropical forests than grassy biomes. Consequently, where loss of tropical forests and their diversity is of wide public concern, loss of grassy vegetation to croplands and plantations has proceeded with little opposition. Indeed afforestation of grasslands is increasingly promoted as a public good (e.g. a means of combating climate change through carbon sequestration).

Nonetheless, TGB contributes significantly to the environmental, economic, and cultural value to the world (Bond and Parr (2010) [5]). TGB stores approximately 15% of the carbon on Earth, account for an estimated 30% of total global terrestrial net primary productivity, represent approximately 85% of the global land area burnt annually, and have a key role in global carbon and energy cycles (Bond and Parr (2010) [5] and references therein). TGB are home to most of the existant mammalian megafauna on Earth, and are the source of origin for important grain crops (e.g., millet and sorghum) (Bond and Parr (2010) [5]). An estimated one-fifth of the global human population depends directly on TGB for their livelihoods, including the use of uncleared lands for grazing, fuel wood, food, and medicinal plants (Bond and Parr (2010) [5]).

Modelling of grassland dynamics is usually encompassed in models of tree-grass interactions in savanna ecosystems (Walker et al. (1981) [44], Tilman (1994) [39], Van Langevelde et al. (2003) [40], Accatino et al. (2010) [2], Tchuinté Tamen et al. (2014) [37], (2016) [35], (2017) [36], Yatat et al. (2014) [48], (2017) [47], (2017b) [46] and references therein). See also Tchuinté Tamen et al. (2017b) [38] for an overview of spatially-implicit tree-grass interactions models. In this section, we apply results of section 3 in order to study grassland dynamics subjected to fire events. As it was discussed in Yatat et al. (2017b) [46], in the contexts where fires are frequent (humid savannas), they generally occur in specific periods in the year (Jeffery et al. (2014) [15]), while in protected areas (mesic savannas) fires are often set in the first part of the dry season (Scholes and Walker (1993) [32], Govender et al. (2006) [13], Diouf et al. (2012) [8]). Furthermore, most of available data on fire occurrences are given in terms of fire-return time or fire period (Scholes and Archer (1997) [31], Van Langevelde et al. (2003) [40], Van Wilgen et al. (2004) [41], Abbadie et al. (2006) [1], Sankaran et al. (2008) [30], Accatino et al. (2010) [2], Calabrese et al. (2010) [7], Staver and Bond (2014) [34]). Therefore fire events are taken into account as periodic impulsive events.

Following Yatat et al. (2014) [48], (2017) [47], (2017b) [46], we assume that the grass biomass (G , in $t.ha^{-1}$) evolves following a logistic growth where the carrying capacity is K ($t.ha^{-1}$). Grass biomass originates from the existing grass biomass (intrinsic growth) with the rate γ (yr^{-1}). It decreases with the rate μ (yr^{-1}) due to external disturbances including human activities and herbivory. The fire-induced death rate for grass biomass is denoted by η . f (yr^{-1}) is the fire frequency (see also Tchuinté Tamen et al. (2014) [37], (2016) [35], (2017) [36] for similar assumptions). $\tau = 1/f$ is the length of inter-fire season, i.e. the time between two successive impulsive fire events. Moreover grass biomass experiences local isotropic biomass propagation in space with the rate D ($ha^2.yr^{-1}$). Taking into account all that previous ecological mechanisms leads to the FKPP-like model (6). In this framework, e_u represents the grassland equilibrium while e_0 stands for the bare soil (absence of vegetation) equilibrium (see Lemma 3). Recall that e_u is biologically meaningful when $\mathcal{R} > 1$ and $\mathcal{R}_\tau > 1$. Reader is referred to [Remark 2 in Yatat et al. (2017) [47]] for biological interpretations of these thresholds.

Based on Theorem 1, page 7, one deduces that the fire-prone grassland model has a positive asymptotic spreading speed. Moreover, that spreading speed is characterized as the slowest speed of grassland vs. bare soil traveling wave solutions. The explicit expression of the spreading speed c^* given in (18), page 7 highlights a direct relationship between the period of impulsive fires (τ), the intensity of fire ($1 - \eta$), and the speed of grassland vs. bare soil invasion. Consequently, for vegetation management policies one can shape/manage the speed of the grassland vs. bare soil invasion through the value of the fire frequency.

5 Numerical simulations

In this section we present some numerical simulations of our models based on the nonstandard finite difference method (NSFDM) formalism (see Anguelov et al. (2012) [3] for an overview on NSFDM). Existence of vegetation mosaics involving grasslands/savannas and forests in humid tropical regions is supported by several empirical evidences (see Yatat et al. (2017b) [46] for more details). Moreover, in such regions fire is a major disturbance and its frequency is not expected to be greater than two (Bond and Keeley (2005) [6]). In the sequel parameter values are therefore chosen in order to mimic such regions (see Yatat et al. (2017b) [46] for more details). It is well-known that the proportion of grass biomass that is burned depends mostly on the fire intensity. In the sequel we distinguish two levels of fire-induced death proportion (η) of grass biomass for a given fire intensity. We first consider a low value (20%) and then, a high value (75%).

5.1 The case where $\eta = 0.2$

In this case, one observes fairly similar dynamics with both time-continuous and impulsive fire events (see Figs. 1 and 2). Indeed a transient state is first observed (e.g. $t \in \{1, 3, 10\}$) before the grassland vs. bare soil invasion wave occurs (e.g. $t \in \{15, 20, 30, 40\}$) (see Fig. 2). Moreover, thanks to impulsive fires, temporal periodic behavior is also observed (see Fig. 1).

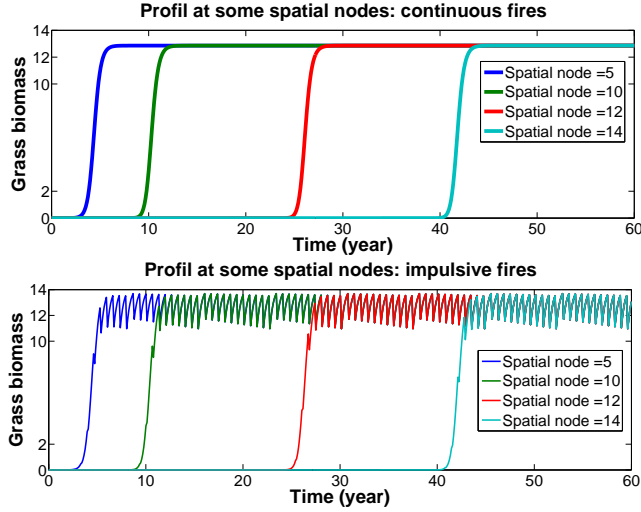


Fig. 1 Profile at different spatial nodes of the fire-prone grassland model with time-continuous (top panel) and impulsive fires (bottom panel). $\gamma = 3.5$, $\mu = 0.2$, $\eta = 0.2$, $K = 15$, $D = 0.001$, $f = 1.5$, $\Delta t = 0.005$ (time-step), $\Delta x = 0.05$ (space-step).

In Fig. 3 we represent level curves of the grassland vs. bare soil spreading speed in the fire-prone grassland model when fires are taken into account as time-continuous or impulsive events. We consider the aforementioned spreading speed as a function of the fire frequency (f) and the biomass diffusion coefficient (D). In addition, in Fig. 4 we observe that for a given value of D , there exists a fire frequency f_0 such that for $f \leq f_0$, the spreading speed with impulsive fires is greater than the spreading speed with time-continuous fires while the reverse holds when $f \geq f_0$. Indeed, by setting $D = 0.001$, we derive Fig. 5 where one observes that the spreading speed decreases with the fire frequency. In other words, reducing the time-between two successive fires leads a decrease of the spreading speed.

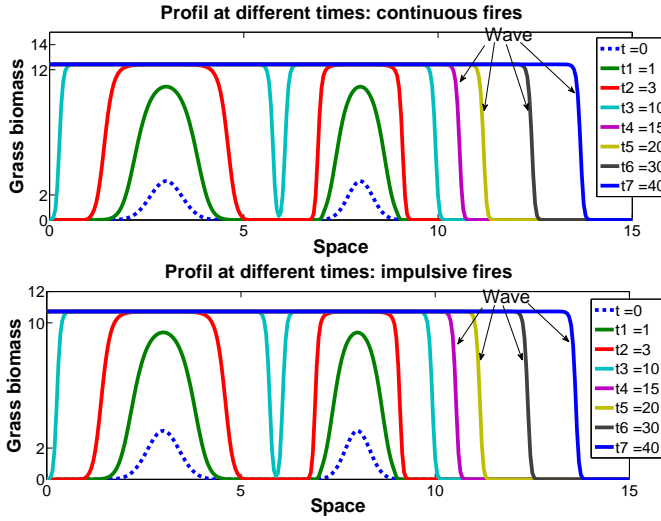


Fig. 2 Profile at different times of the fire-prone grassland model with time-continuous (top panel) and impulsive fires (bottom panel). $\gamma = 3.5$, $\mu = 0.2$, $\eta = 0.2$, $K = 15$, $D = 0.001$, $f = 2$, $\Delta t = 0.005$ (time-step), $\Delta x = 0.05$ (space-step).

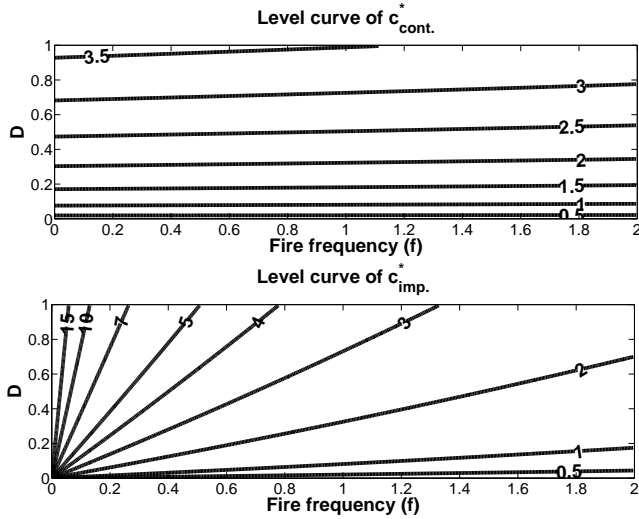


Fig. 3 Level curves of the grassland vs. bare soil spreading speed as a function of fire frequency (f) and biomass diffusion coefficient (D) with time-continuous fires (top panel) and impulsive fires (bottom panel). $\gamma = 3.5$, $\mu = 0.2$, $\eta = 0.2$, $K = 15$.

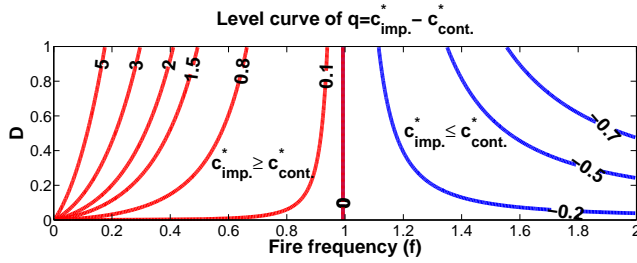


Fig. 4 Level curves of the difference of grassland vs. bare soil spreading speed as a function of f and D , experiencing impulsive or time-continuous fires. $\gamma = 3.5$, $\mu = 0.2$, $\eta = 0.2$, $K = 15$. Red lines correspond to $c_{imp}^* \geq c_{cont}^*$, blue lines correspond to $c_{imp}^* \leq c_{cont}^*$, while the purple line corresponds to $c_{imp}^* = c_{cont}^*$.

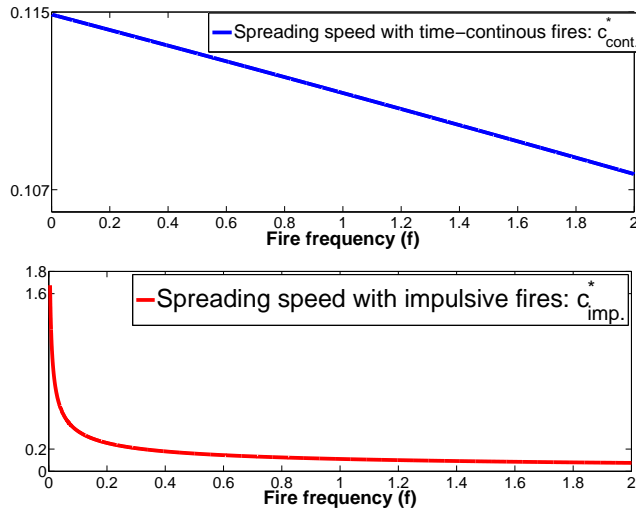


Fig. 5 Grassland vs. bare soil spreading speed in the fire-prone grassland model with time-continuous fires (top panel) and impulsive fires (bottom panel). $\gamma = 3.5$, $\mu = 0.2$, $\eta = 0.2$, $K = 15$, $D = 0.001$.

5.2 The case where $\eta = 0.75$

In this case, one observes contrasting dynamics when time-continuous and impulsive fire events are considered (see Figs. 6, 7 and 8). Indeed in the case of time-continuous fires, the wave is rapidly reached (e.g. $t = 20$ in the top panel of Fig. 8) in comparison with the impulsive counterpart ($t = 50$ in the bottom panel of Fig. 8). Therefore, with a relative high value of the fire-induced death rate, the wave rapidly

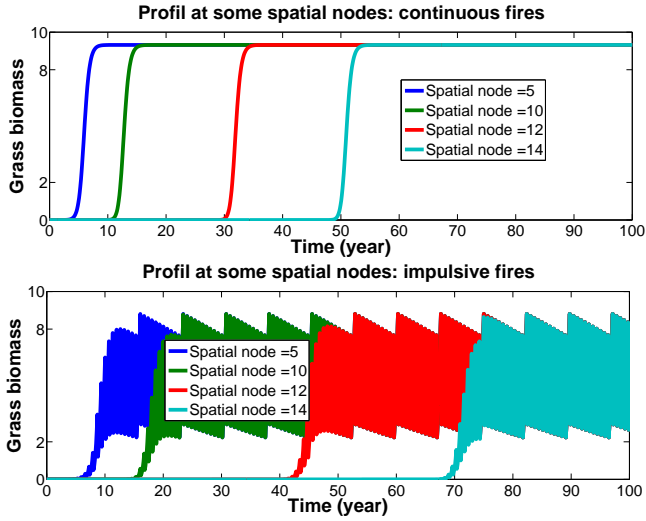


Fig. 6 Profile at different spatial nodes of the fire-prone grassland model with time-continuous fires (top panel) and impulsive fires (bottom panel). $f = 1.5$, $\gamma = 3.5$, $\mu = 0.2$, $\eta = 0.75$, $K = 15$, $D = 0.001$, $\Delta t = 0.005$ (time-step), $\Delta x = 0.05$ (space-step).

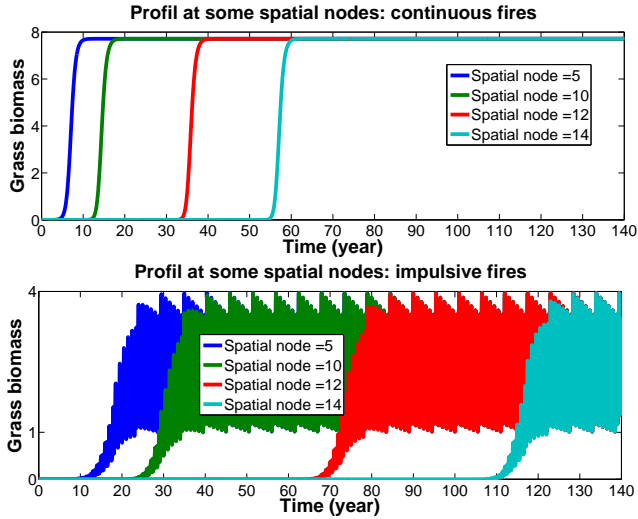


Fig. 7 Profile at different spatial nodes of the fire-prone grassland model with time-continuous fires (top panel) and impulsive fires (bottom panel). $f = 2$, $\gamma = 3.5$, $\mu = 0.2$, $\eta = 0.75$, $K = 15$, $D = 0.001$, $\Delta t = 0.005$ (time-step), $\Delta x = 0.05$ (space-step).

takes place when time-continuous fires are considered. Conversely, the wave takes more time to occur when periodic impulsive fires are considered. As in Fig. 1, thanks

to impulsive fires, temporal periodic behavior is also observed but the amplitude of the periodic behavior is more consequent in this case (see Figs. 6 and 7).

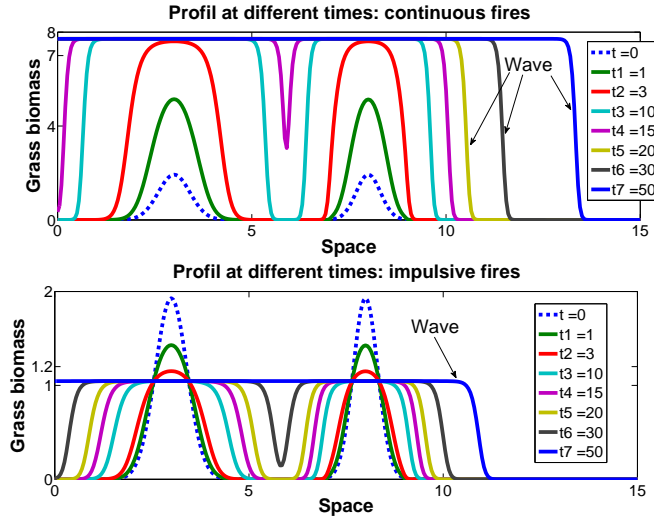


Fig. 8 Profile at different times of the fire-prone grassland model with time-continuous fires (top panel) and impulsive fires (bottom panel). $\gamma = 3.5$, $\mu = 0.2$, $\eta = 0.75$, $K = 15$, $D = 0.001$, $f = 2$, $\Delta t = 0.005$ (time-step), $\Delta x = 0.05$ (space-step).

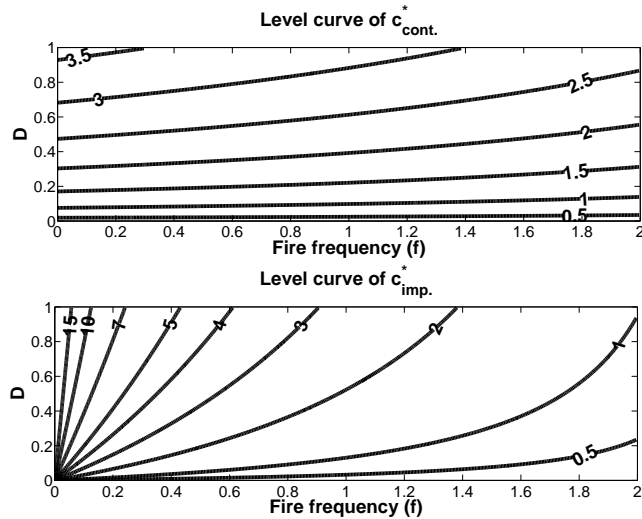


Fig. 9 Level curves of the grassland vs. bare soil spreading speed as a function of fire frequency (f) and biomass diffusion coefficient (D) with time-continuous fires (top panel) and impulsive fires (bottom panel). $\gamma = 3.5$, $\mu = 0.2$, $\eta = 0.75$, $K = 15$.

Similarly as in Fig. 3, we represent level curves of the grassland vs. bare soil spreading speed in the fire-prone grassland model as a function of f and D (see Fig. 9). Moreover, from Fig. 10 we deduce that f_0 exists for a given value of the diffusion coefficient D (see also Fig. 4). Furthermore, in the particular case where $D = 0.001$, a decrease of the spreading speed with the fire frequency is depicted in Fig. 11.

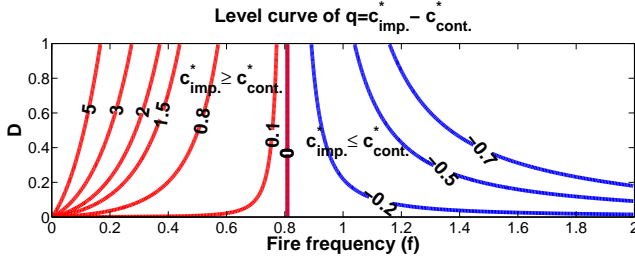


Fig. 10 Level curves of the difference of grassland vs. bare soil spreading speed as a function of f and D , experiencing impulsive or time-continuous fires. $\gamma = 3.5$, $\mu = 0.2$, $\eta = 0.75$, $K = 15$. Red lines correspond to $c_{imp.}^* \geq c_{cont.}^*$, blue lines correspond to $c_{imp.}^* \leq c_{cont.}^*$ while the purple line corresponds to $c_{imp.}^* = c_{cont.}^*$.

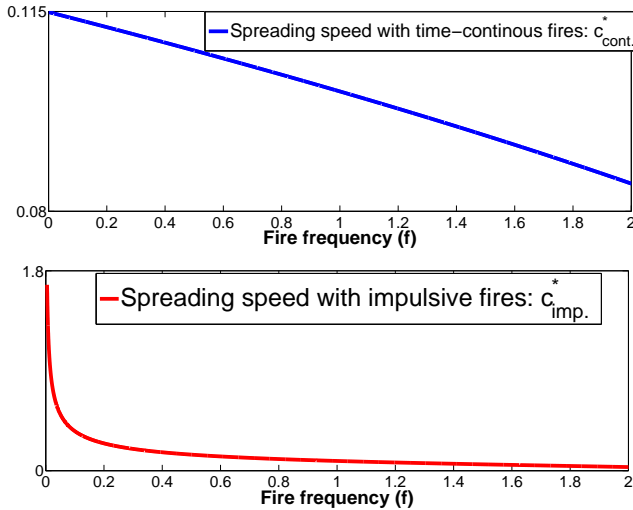


Fig. 11 Grassland vs. bare soil spreading speed of the fire-prone grassland model with time-continuous fires (top panel) and impulsive fires (bottom panel). $\gamma = 3.5$, $\mu = 0.2$, $\eta = 0.75$, $K = 15$.

6 Conclusion-discussion

In this paper we considered a classic and well-known reaction-diffusion scalar equation taking into account periodic impulsive events.

Based on recursion equation proposed by Weinberger (1982) [45] and using results of Lewis and Li (2012) [19] we derived an explicit expression of the population vs. extinction spreading speed. We carried out a comparison with the time-continuous counterpart and showed that depending on the value of the time between two successive impulsive events, the spreading speed with impulsive events can be greater, equal or lower than the spreading speed with time-continuous events. In addition, we applied our results in order to get some insights for fire-prone grassland dynamics. We found that the time between two successive fires has the potential to shape the speed of the grassland vs. bare soil invasion. Moreover, depending on the magnitude of the fire-induced death rate η , the fire-prone grassland model with either time-continuous or impulsive fires experiences fairly similar dynamics (e.g. low values of η) or contrasted dynamics (e.g. high values of η).

This paper is a first step towards a more general study to characterize the existence of travelling wave solutions for a system of reaction-diffusion equations with impulses.

Acknowledgements

VY is grateful to the organizing committee of the International Conference on Mathematical Methods and Models in Biosciences (BIOMATH) 2017 for financial support that allows him to attend the conference in Skukuza Camp, Kruger Park, South Africa, 25-30 June 2017.

References

1. L. Abbadie, J. Gignoux, X. Le Roux, and M. Lepage. *Lamto: structure, functioning, and dynamics of a Savanna Ecosystem*. Springer, 2006.
2. F. Accatino, C. De Michele, R. Vezzoli, D. Donzelli, and R. Scholes. Tree-grass co-existence in savanna: interactions of rain and fire. *J. Theor. Biol.*, 267:235–242, 2010.
3. R. Anguelov, Y. Dumont, and J.M. Lubuma. On nonstandard finite difference schemes in biosciences. *AIP Conf. Proc.*, 1487:212–223, 2012.
4. D.D. Bainov and P.S. Simeonov. *Impulsive Differential Equations: Asymptotic properties of the solutions*. World Scientific Publishing Co., 1995.
5. W.J. Bond and C.J. Parr. Beyond the forest edge: Ecology, diversity and conservation of the grassy biomes. *Biol. Conserv.*, 143:2395–2404, 2010.
6. W.J. Bond, F.I. Woodward, and G.F. Midgley. The global distribution of ecosystems in a world without fire. *New Phytol.*, 165:525–538, 2005.
7. J.M. Calabrese, F. Vazquez, C. López, M. San Miguel, and V. Grimm. The independent and interactive effects of tree-tree establishment competition and fire on savanna structure and dynamics. *Am. Nat.*, 175:E44–E65, 2010.

8. A. Diouf, N. Barbier, A.M. Lykke, P. Couteron, V. Deblauwe, A. Mahamane, M. Saadou, and J. Bogaert. Relationships between fire history, edaphic factor and woody vegetation structure and composition in a semi-arid savanna landscape (niger, west africa). *Appl. Veg. Sci.*, 15:488–500, 2012.
9. C. Dufourd and Y. Dumont. Impact of environmental factors on mosquito dispersal in the prospect of sterile insect technique control. *Computers & Mathematics with Applications*, 66(9):1695 – 1715, 2013. BioMath 2012.
10. Y. Dumont and J. M. Tchuente. mathematical studies on the sterile insect technique for the chikungunya disease and aedes albopictus. *J. Math. Biol.*, 65 (5):809–854, 2012.
11. M. Fazly, M. Lewis, and H. Wang. On impulsive reaction-diffusion models in higher dimensions. *SIAM J. Appl. Math.*, 77(1):224–246, 2017.
12. R.A. Fisher. The wave of advantageous genes. *Ann. Eugen.*, 7:255–369, 1937.
13. N. Govender, W.S.W. Trollope, and B.W. Van Wilgen. The effect of fire season, fire frequency, rainfall and management on fire intensity in savanna vegetation in south africa. *J. Appl. Ecol.*, 43(4):748–758, 2006.
14. Q. Huang, H. Wang, and M.A. Lewis. A hybrid continuous/discrete-time model for invasion dynamics of zebra mussels in rivers. *SIAM J. Appl. Math.*, 77(3):854–880, 2017.
15. K.J. Jeffery, L. Korte, F. Palla, G. Walters, L.J.T. White, and K.A. Abernethy. Fire management in a changing landscape: a case study from lope national park, gabon. *Parks*, 20:39–52, 2014.
16. M. Kirane and Y. Rogovchenko. Comparison results for systems of impulse parabolic equations with applications to population dynamics. *Nonlin. Ana.: Theo., Meth. & Appl.*, 28(2):263 – 276, 1997.
17. A.N. Kolmogorov, I.G. Petrowsky, and N.S. Piscounov. Étude de léquation de la diffusion avec croissance de la quantité de matière et son application à un problème biologique. *Bull. Univ. État Mosc., Ser. Int., A*, 1:1–26, 1937.
18. V. Lakshmikantham, D.D. Bainov, and P.S. Simeonov. *Theory of Impulsive Differential Equations*. World Scientific, Singapore, 1989.
19. M.A. Lewis and B. Li. Spreading speed, traveling waves, and minimal domain size in impulsive reaction–diffusion models. *Bull. Math. Biol.*, 74(10):2383–2402, Oct 2012.
20. J.D. Logan. *An introduction to nonlinear partial differential equations, second edition*. John Wiley and Sons, Inc., 2008.
21. J.D. Logan. *Applied Partial Differential Equations*. Undergraduate Texts in Mathematics. Springer International Publishing, 3 edition, 2015.
22. Z. Ma and J. Li. *Dynamical Modeling and Analysis of Epidemics*. World Scientific Publishing Co. Pte. Ltd. Singapore., 2009.
23. A. Okubo and S. Levin. *Diffusion and ecological problems*. Springer, 2001.
24. C.L. Parr, C.E.R. Lehmann, W.J. Bond, W.A. Hoffmann, and A.N. Andersen. Tropical grassy biomes: misunderstood, neglected, and under threat. *Trends in Ecol. and Evol.*, 29(4):205–213, April 2014.
25. B. Perthame. *Parabolic Equations in Biology*. Lecture Notes on Mathematical Modelling in the Life Sciences. Springer, 2015.
26. M. H. Protter and H. F. Weinberger. *Maximum principles in differential equations*. Springer, 1984.
27. Y. Rogovchenko. Impulsive evolution systems: Main results and new trends. *Dyn. Cont. Disc. Imp. Sys.*, 3:57–88, 1997.
28. Y. Rogovchenko. Nonlinear impulsive evolution systems and applications to population models. *J. Math. Anal. and Appl.*, 207:300–315, 1997.
29. M. Sankaran, N.P. Hanan, R.J. Scholes, J. Ratnam, DJ. Augustine, B.S. Cade, J. Gignoux, S.I. Higgins, X. LeRoux, F. Ludwig, J. Ardo, F. Banyikwa, A. Bronn, G. Bucini, K.K. Caylor, M.B. Coughenour, A. Diouf, W. Ekaya, C.J. Feral, E.C. February, P.G.H. Frost, P. Hiernaux, H. Hrabar, K.L. Metzger, H.H.T. Prins, S. Ringrose, W. Sea, J. Tews, J. Worden, and N. Zambatis. Determinants of woody coverin african savannas. *Nature*, 438:846–849, 2005.
30. M. Sankaran, J. Ratnam, and N. Hanan. Woody cover in african savannas: the role of resources, fire and herbivory. *Global Ecol. Biogeogr.*, 17(2):236–245, 2008.

31. R.J. Scholes and S.R. Archer. Tree-grass interactions in savannas. *Annu. Rev. Ecol. Syst.*, 28:517–544, 1997.
32. R.J. Scholes and B. Walker. *An African Savanna: Synthesis of the Nylsvley Study*. Cambridge University Press, Cambridge, 1993.
33. N. Shigesada and K. Kawasaki. *Biological invasions: theory and practice*. Oxford series in ecology and evolution. Oxford University Press, 1997.
34. A.C. Staver and W.J. Bond. Is there a browse trap ? dynamics of herbivore impacts on trees and grasses in an african savannas. *J. Eco.*, 102:595–602, 2014.
35. A. Tchuinté Tamen, Y. Dumont, J. J. Tewa, S. Bowong, and P. Couteron. Tree-grass interaction dynamics and pulsed fires: mathematical and numerical studies. *Appl. Math. Mod.*, 40(11-12):6165–6197, June 2016.
36. A. Tchuinté Tamen, Y. Dumont, J. J. Tewa, S. Bowong, and P. Couteron. A minimalistic model of tree-grass interactions using impulsive differential equations and non-linear feedback functions of grass biomass onto fire-induced tree mortality. *Math. Comput. Simul.*, 133:265–297, March 2017.
37. A. Tchuinté Tamen, J. J. Tewa, P. Couteron, S. Bowong, and Y. Dumont. A generic modeling of fire impact in a tree-grass savanna model. *Biomath.*, 3:1407191, 2014.
38. A. Tchuinté Tamen, V. Yatata, Y. Dumont, and P. Couteron. A tribute to the use of minimalistic spatially-implicit models of savanna vegetation dynamics to address broad spatial scales in presence of scarce data. *Submitted*, 2017.
39. D. Tilman. Competition and biodiversity in spatially structured habitats. *Ecology*, 75(1):2–16, 1994.
40. F. Van Langevelde, C. Van de Vijver, L. Kumar, J. Van de Koppel, N. De Rider, and J. Vanandel. Effects of fire and herbivory on the stability of savanna ecosystems. *Ecology*, 84(2):337–350, 2003.
41. B.W. Van Wilgen, N. Govender, H.C. Biggs, D. Ntsala, and X.N. Funda. Response of savanna fire regimes to changing fire-management policies in a large african national park. *Conserv. Biol.*, 18:1537–1540, 2004.
42. O. Vasilyeva, F. Lutscher, and M. Lewis. Analysis of spread and persistence for stream insects with winged adult stages. *J. Math. Biol.*, 72(4):851–875, Mar 2016.
43. V. Volpert. *Elliptic Partial Differential Equations: Volume 2 Reaction-Diffusion Equations*. Springer, 2014.
44. B. Walker, D. Ludwig, C.S. Holling, and R.M. Peterman. Stability of semi-arid savanna grazing systems. *J. Ecol.*, 69(2):473–498, 1981.
45. H. F. Weinberger. Long-time behavior of a class of biological models. *SIAM J. Math. Anal.*, 13(3):353–396, 1982.
46. V. Yatata, P. Couteron, and Y. Dumont. Spatially explicit modelling of tree-grass interactions in fire-prone savannas: a partial differential equations framework. *Ecol. Complexity*, pages –, 2017.
47. V. Yatata, P. Couteron, J. J. Tewa, S. Bowong, and Y. Dumont. An impulsive modelling framework of fire occurrence in a size-structured model of tree–grass interactions for savanna ecosystems. *J. Math. Biol.*, 74(6):1425–1482, 2017.
48. V. Yatata, Y. Dumont, J. J. Tewa, P. Couteron, and S. Bowong. Mathematical analysis of a size structured tree-grass competition model for savanna ecosystems. *Biomath.*, 3:1404212, 2014.
49. S. Zheng. A reaction-diffusion system of a predator-prey-mutualist model. *Math. Biosc.*, 78:217–245, 1986.
50. S. Zheng. A reaction-diffusion system of a competitor-competitor-mutualist model. *J. Math. Ana. Appl.*, 124:254–280, 1987.
51. S. Zheng. *Nonlinear evolution equations*. Chapman & Hall/CRC, 2004.

Appendix A: proof of Lemma 1

Let us set $\mathcal{S} = \frac{\gamma}{\mu + f\eta + D\lambda_1}$ where $\lambda_1 = \frac{\pi^2}{l^2}$. Following the proof of Theorem 4.3 of Zheng (1986) [49] (see also Theorem 3.3 of Zheng (1987) [50]) one deduces that if $\mathcal{S} < 1$ then $E_0 = 0$, the trivial equilibrium of (4)-(2)-(8) is globally asymptotically stable i.e., $\lim_{t \rightarrow +\infty} G(t, x) = 0$. Recall that $\mathcal{S} < \mathcal{R}^{cont.}$ where $\mathcal{R}^{cont.} = \frac{\gamma}{\mu + f\eta}$. In

addition, when $\mathcal{R}^{cont.} > 1$, one has $\mathcal{S} < 1 \Leftrightarrow l < l_{cont.}^* = \pi \sqrt{\frac{D}{(\mu + f\eta)(\mathcal{R}^{cont.} - 1)}}$.

Therefore, part 1.a. of Lemma 1 holds.

Based on Theorem 4.4 of Zheng (1986) [49] (see also Theorem 3.4 of Zheng (1987) [50]) and by using the concept of upper/lower solution one proves that when $l > l_{cont.}^*$, system (4)-(2)-(8) admits a positive equilibrium $\bar{G}(x)$. In addition following the proof of Theorem 6.3.1 of Zheng (2004) [51] one can prove that $\lim_{t \rightarrow +\infty} G(t, x) = \bar{G}(x)$. This achieves the proof of part 1.b. of Lemma 1.

Part 2 of Lemma 1 is done following the proof of Theorem 3.1 of Lewis and Li (2012) [19], with $g(x) = (1 - \eta)x$.

Appendix B: proof of Lemma 3

Let us denote by F the right hand side of model (14).

$$F'(u) = \frac{K^2(\mu - \gamma)^2(1 - \eta)e^{(\mu - \gamma)\tau}}{(K(\mu - \gamma)e^{(\mu - \gamma)\tau} + u\gamma(1 - \eta)(e^{(\mu - \gamma)\tau} - 1))^2}.$$

Therefore, $F'(0) = \frac{(1 - \eta)}{e^{-\mu(\mathcal{R} - 1)\tau}} = \mathcal{R}_\tau$. Consequently for $\mathcal{R} < 1$ (with relation (15)) or $\mathcal{R}_\tau < 1$, the trivial equilibrium $e_0 = 0$ is GAS. The first part holds. Positive equilibria u of model (14) satisfy

$$u = \frac{K(\mu - \gamma)u}{(K(\mu - \gamma) + \gamma u)e^{(\mu - \gamma)\tau} - \gamma u}.$$

After direct computation one obtains

$$e_u = \frac{K(\mathcal{R} - 1)(\mathcal{R}_\tau - 1)}{\mathcal{R}(\mathcal{R}_\tau - 1 + \eta)}.$$

Equilibrium e_u is biologically meaningful whenever $\mathcal{R} > 1$ and $\mathcal{R}_\tau > 1$. Moreover,

$$\begin{aligned}
F'(e_u) &= \frac{K^2(\mu - \gamma)^2(1 - \eta)e^{(\mu - \gamma)\tau}}{(K(\mu - \gamma)e^{(\mu - \gamma)\tau} + u\gamma(1 - \eta)(e^{(\mu - \gamma)\tau} - 1))^2} \\
&= \frac{K^2(\mu - \gamma)^2(1 - \eta)e^{(\mu - \gamma)\tau}}{(e^{(\mu - \gamma)\tau})^2(K(\mu - \gamma) + e_u\gamma(1 - \eta)(1 - e^{-(\gamma - \mu)\tau}))^2} \\
&= \frac{\mathcal{R}_\tau K^2(\mu - \gamma)^2}{(K(\mu - \gamma) + e_u\gamma(1 - \eta - \mathcal{R}_\tau))^2} \\
&= \frac{\mathcal{R}_\tau K^2(\gamma - \mu)^2}{(K(\gamma - \mu) + e_u\gamma(\mathcal{R}_\tau - 1 + \eta))^2}.
\end{aligned} \tag{24}$$

Substituting e_u in (24) leads that

$$\begin{aligned}
F'(e_u) &= \frac{\mathcal{R}_\tau K^2(\gamma - \mu)^2}{(K(\gamma - \mu) + K(\gamma - \mu)(\mathcal{R}_\tau - 1))^2} \\
&= \frac{\mathcal{R}_\tau K^2(\gamma - \mu)^2}{(K(\gamma - \mu)\mathcal{R}_\tau)^2} \\
&= \frac{1}{\mathcal{R}_\tau}.
\end{aligned} \tag{25}$$

Since $\mathcal{R}_\tau > 1$, one deduces from (25) that $|F'(e_u)| < 1$. That is equilibrium e_u is GAS. This ends the proof.